

https://doi.org/10.1070/QEL18005

Backward SRS suppression of picosecond pulses in water upon moving the pump beam waist from the water volume through the surface

S.M. Pershin, A.I. Vodchits, I.A. Khodasevich, V.A. Orlovich,
A.D. Kudryavtseva, N.V. Tcherniega

Abstract. **We report, for the first time to our knowledge, suppression of backward stimulated Raman scattering (BSRS) of picosecond pulses (57 ps, 532 nm) due to the development of optical breakdown in the surface (0–3 mm) water layer with a shift of the beam waist (lens focal length of 83 mm) to the water–air interface without changing the pump pulse energy (~1.3–1.5 mJ). In this case, SRS generation in forward direction is observed even in the presence of breakdown. When the focal plane coincides with the surface, the BSRS generation is restored without optical breakdown, despite an increase in the pump radiation intensity due to a decrease in the beam diameter. It is significant that the optical breakdown threshold in the water volume was unattainable even with an increase in the pump pulse energy by more than an order of magnitude – up to 16 mJ. The mechanism of self-consistent summation of nonlinear optical processes, such as electrostriction, beam self-focusing, beam phase conjugation, and BSRS pulse compression is discussed.**

Keywords: *backward and forward SRS of picosecond pulse in water, water–air interface, beam waist, surface spallation.*

1. Introduction

It is known that the first (1961) nonlinear optical frequency converter of laser radiation was a Franken second harmonic generator based on a quartz crystal [1]. In the first monograph on nonlinear optics [2], its basic principles were developed, and the existing and future nonlinear optical laser frequency converters were analysed as sources of coherent radiation in new spectral ranges. Along with harmonic generators, sum and difference frequencies, in which the frequency tuning step is determined by the quantum of pump laser radiation, the most well-known were frequency converters based on stimulated Raman scattering (SRS) on natural vibrations of molecules, or Raman lasers [3, 4].

The frequency shift in the Raman converter (in both directions from the pump laser radiation frequency when generating several components) is equal to the quantum of the vibrational transition energy in a transparent sample: gas, liquid, or solid [5]. Note that this frequency shift was an order of magnitude smaller than in harmonic generators [1, 2], and had a large, almost unlimited set of frequencies, mainly depending on the mass of substance molecules [6, 7]. For example, the frequency shift of SRS components in hydrogen was ~4155 cm^{-1}; in water, ~3450 cm^{-1}; in methane, ~2917 cm^{-1}; in nitrogen, ~2329 cm^{-1}; and in oxygen, ~1555 cm^{-1}. It should also be noted that in water, despite a large shift, the SRS threshold in the field of nanosecond pulses was not reached due to optical breakdown [8].

In liquid nitrogen, on the contrary, the SRS threshold turned out to be low. At the same time, several interesting features of the development of high conversion efficiency SRS were discovered in nitrogen due to the energy jump of Stokes pulses (by seven orders of magnitude) and the asymmetry of amplification in the forward and backward directions [3, 4]. In liquid nitrogen, SRS was first implemented in a parallel pump beam [9] with spontaneous activation of a resonator via distributed feedback due to Rayleigh scattering [10], generation of terahertz radiation in the field of femtosecond pulses [11] was obtained, and a decrease in the SRS threshold of picosecond pulses was detected by focusing pump radiation near the surface as compared to focusing in the volume [12].

Transition to picosecond pump pulses made it possible to overcome the SRS threshold in water without optical breakdown [13, 14] upon focusing the pump beam in the volume of water. Moreover, relatively recently [15–18], a new interesting phenomenon was discovered: a multiple (up to 30 times) decrease in the SRS threshold of picosecond pulses in water upon moving the beam waist from the volume of water through the surface into the air. Based on work [9], we explained the observed phenomenon as the activation of an asymmetric resonator formed by distributed feedback (DFB) [10] in the volume of water and a concentrated mirror – a surface with Fresnel reflection (2%), which is many orders of magnitude greater than the retroreflectivity under DFB [12].

However, it remained unclear how the asymmetry of forward SRS radiation (in the forward direction, FSRS) and backward SRS radiation (in the backward direction, BSRS) [13], as well as the SRS conversion efficiency, change when the pump beam waist crosses the water surface without reducing the energy of its pulses, despite lowering the SRS threshold [15–17]. The study of this issue was the aim of this work.

BSRS was discovered almost simultaneously with the discovery of the forward SRS in the 1960s. In a number of works [19–21], the main physical properties of BSRS were investigated upon focusing the pump beam into the sample volume. It was shown that, in the case of BSRS, the Stokes pulse dura-

S.M. Pershin Prokhorov General Physics Institute of the Russian Academy of Sciences, ul. Vavilova 38, 119991 Moscow, Russia; e-mail: pershin@kapella.gpi.ru;
A.I. Vodchits, I.A. Khodasevich, V.A. Orlovich B.I. Stepanov Institute of Physics of the National Academy of Sciences of Belarus, prosp. Nezavisimosti 68-2, 220072 Minsk, Republic of Belarus; e-mail: a.vodchits@dragon.bas-net.by, orlovich@dragon.bas-net.by;
A.D. Kudryavtseva, N.V. Tcherniega Lebedev Physical Institute of the Russian Academy of Sciences, Leninsky prosp. 53, 119991 Moscow, Russia

Received 30 November 2021
Kvantovaya Elektronika **52** (3) 283–288 (2022)
Translated by M.A. Monastyrskiy

tion is significantly reduced compared to that in the case of FSRS, and a high conversion efficiency (in terms of power) of pump radiation into Stokes radiation can be attained.

Subsequently, a number of BSRS studies were performed in compressed gases, liquids, plasma, optical fibre, and other media [22–32]. One can observe an asymmetry in the properties of BSRS and FSRS in the process of the SRS development. Under special conditions of SRS excitation (tight focusing of exciting radiation into the medium), it is possible to achieve a high conversion efficiency into the Stokes component of the BSRS and almost complete suppression of the FSRS process [30]. A significant reduction in the BSRS Stokes pulse duration compared to the duration of the pump pulse is used in ultrashort pulse compressors based on BSRS radiation frequency converters. The beam phase conjugation is also observed in the BSRS process [33, 34], which is of great applied significance.

It is very important to study the BSRS characteristics in water. Some properties of water do not yet have a convincing explanation (in particular, the properties of water near the interface, for example, the structure of ice in the water layer at room temperature [35] or a higher value of the order parameter in the near-surface water layer compared to that on the ice surface [36]). A number of studies on BSRS in water have been already performed (see, for example, [29]). The general direction of such studies is to optimise BSRS and to achieve a high efficiency of pump radiation conversion into the radiation of the first Stokes component. Recently, studies of the influence of phase boundaries (liquid–plasma, liquid–gas, etc.) on nonlinear optical processes, including on SRS [37, 16, 17], have become relevant. However, no systematic studies of BSRS in water have actually been performed.

This paper presents the results of studying SRS of picosecond radiation pulses in water in the vicinity of the water–air interface: threshold and energy characteristics of BSRS and FSRS as functions of the pump beam waist position relative to the water surface. Preliminary spectral measurements were also carried out.

2. Experiment

The optical scheme of the experiment is shown in Fig. 1. The pump radiation (Lotis TII laser, wavelength 532 nm, pulse duration 57 ps, repetition rate 15 Hz) was deflected rightwards by a dichroic mirror M onto a prism P, which directed the beam vertically down onto a lens L1 with a focal length of 83 mm, focusing the pump radiation onto the sample. Distilled water was placed in a cell with a diameter of 20 mm and a length of 75 mm with a transparent bottom and an open surface. The cell was placed on a table to move it vertically up and down in 0.1 mm increments. The initial position of the cell was chosen so that the beam waist was in the water at a distance of 15 mm from the surface and approached the surface as the cell was moving down.

A lens L2 was installed behind the cell to collimate the FSRS and pump beams. Optical filters F were used to select FSRS radiation. After passing through the filters, the FSRS beam was incident either on a white screen S for visual observation and spectrum measurement, or on a detector for measuring the energy of the FSRS pulses. The BSRS radiation beam passed through a folding mirror M with a transmittance of at least 85%–90% at a wavelength of 652 nm of the first Stokes component. Below the mirror, a focusing lens, a Pellin–Broca prism with a 90-degree deviation, and filters F

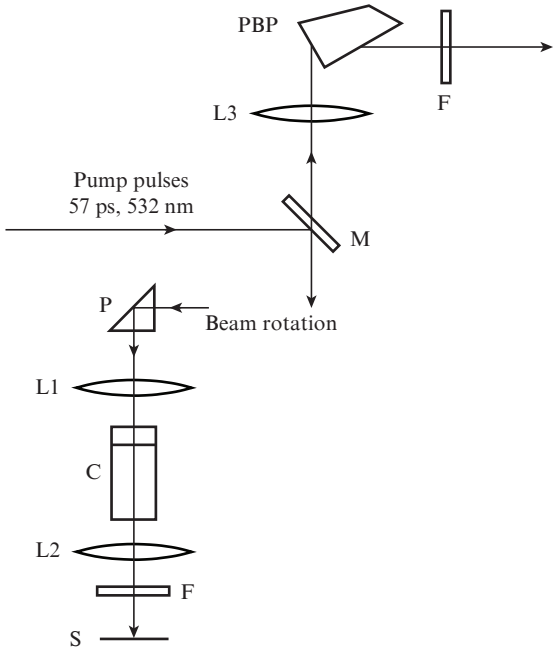

Figure 1. Optical scheme of the experiment (upper part – top view, lower part – side view):
(M) mirror; (L1, L2, and L3) focusing lenses; (PBP) Pellin–Broca prism; (F) optical filters; (P) prism; (C) water cell; (S) screen.

were installed to select and direct BSRS beam to a pulse energy meter or to a spectrometer slit.

The pump radiation beam with a diameter of ~8 mm and a Gaussian intensity distribution over the cross section had a divergence of ~0.4–0.6 mrad and linear polarisation in the horizontal plane. An attenuator made of two Glan prisms was introduced into the pump beam to vary the pump energy in the range of 0.1–16 mJ. The beam diameter ($2\omega_0$) at the waist was ~40 μm. Then the length of the confocal parameter of the beam (caustic surface), or doubled Rayleigh length

$$2L_R = (2\pi\omega_0^2)/\lambda, \quad (1)$$

can be roughly estimated as 4.8 mm for pump radiation with $\lambda = 0.532$ μm. Note that at the maximum pump pulse energy (~16 mJ), the radiation intensity in the focal plane reached ~20 TW cm^{-2}, but was below the threshold intensity of multiphoton ionisation of water (~40 TW cm^{-2}) in the field of picosecond pulses of the second harmonic of a neodymium laser [8]. We have not reached the optical breakdown threshold in the water volume upon focusing pump radiation with a close-to-maximum energy. The energy of the pump pulses, as well as of the FSRS and BSRS pulses was measured with an IMO-2N power meter, and the SRS spectra were measured using an S100 mini-spectrometer with a fibre input.

3. Results and discussion

Figure 2 shows the dependences of the pulse energy E_{SRS} of the first Stokes component at a wavelength of 652 nm (the Stokes shift is ~3450 cm^{-1}) for FSRS and BSRS radiation on the pump pulse energy E_p. The measurements were carried

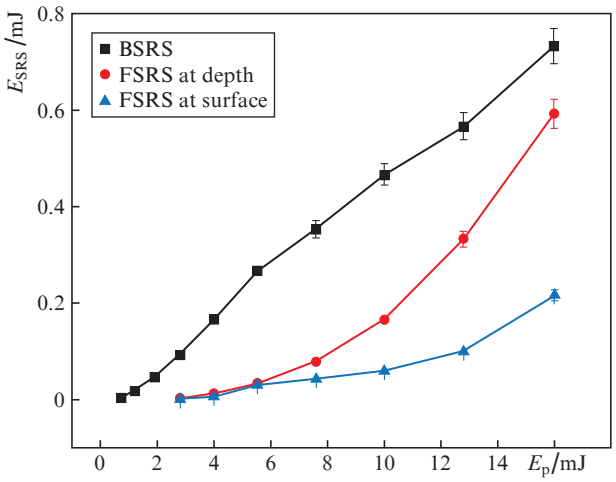

Figure 2. (Colour online) Dependence of the energy of BSRS and FSRS pulses in water on the pump pulse energy and the pump beam waist position.

out by focusing the pump radiation into the depth of the cell at a distance of 15 mm from the water surface and at the water–air interface.

Figure 3 shows the results of evaluating the efficiency of converting the energy of pump pulses into SRS components. Experimental data are presented without allowance for losses on optical elements. One can see that BSRS undergoes a transition to the saturation regime at pump pulse energies above 5–6 mJ. With allowance for the radiation losses on the optical elements, the maximum efficiency of converting pump radiation into BSRS components reaches ~12%, and into the FSRS components, about 8%.

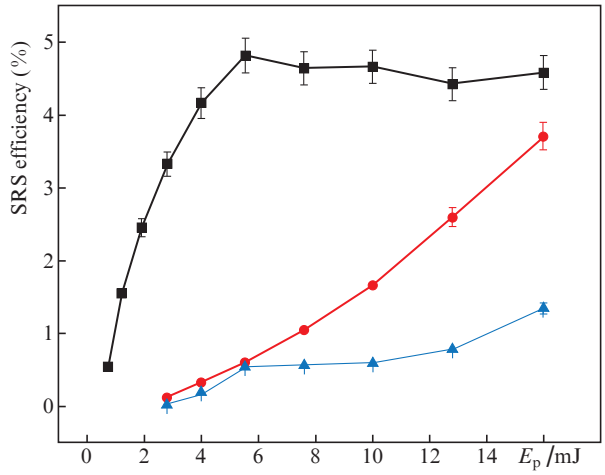

Figure 3. (Colour online) Dependences of BSRS and FSRS efficiency in water on the pump pulse energy E_p (■ – BSRS; ● – FSRS, beam waist in the water volume; ▲ – FSRS, beam waist near the water-air interface).

Figure 4 shows the SRS threshold dependences in the forward and backward directions on the beam waist distance to the water–air interface. The SRS threshold energy was recorded on a screen when a red spot of the Stokes component appeared at a wavelength of 652 nm. One can see that when the beam waist moves in the volume of water, both dependences have the same areas with constant (at a depth of more than 9 mm) and with slightly increasing (from 0.39 to 0.43 mJ at a depth of 7–5 mm) threshold energies, and then, as the beam waist approaches the surface, areas with an increase in the threshold and dramatic differences between these energies.

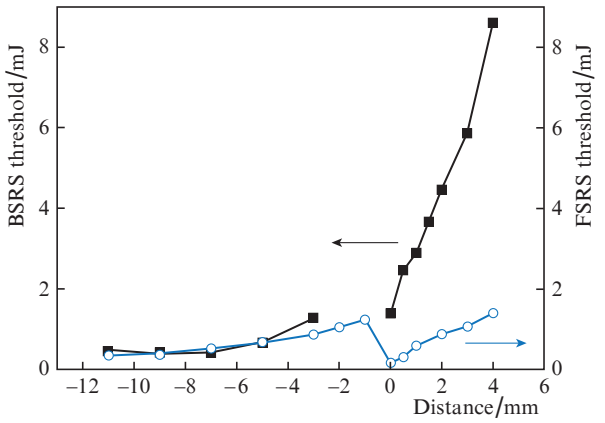

Figure 4. (Colour online) Dependences of the threshold values of BSRS (■) and FSRS (○) on the beam waist distance to the water surface. Negative values along the abscissa axis correspond to the beam waist positions in the water volume, and zero, to alignment with the water surface.

Thus, the FSRS threshold repeats the N-shaped dependence, but with a 7-fold decrease in energy (up to ~0.17 mJ) near the surface, which we first detected earlier in water [15] and liquid nitrogen [12] in the field of pulses with a duration of 15 ps. We should note here that the similarity of the N-shaped dependences indicates the fundamental nature of the discovered phenomenon and confirms the mechanism proposed in [15] for the surface to act as a concentrated mirror of an asymmetric distributed feedback resonator [9, 10] in the water volume. The last section of the SRS threshold growth when the beam is removed from the surface into the air for both SRS components clearly demonstrates an N-shaped dependence. The observed increase in the SRS threshold with a decrease in the beam waist depth, starting from a depth of 5–7 mm (Fig. 4), may be associated with the onset of a reduction in the gain length in the exponent index when the upper part of the caustic surface emerges from the water into the air, assuming that the SRS gain g remains constant. It is known [6–8, 30, 38] that the gain increment G in the exponent index of the radiation intensity growth of the SRS Stokes component is determined by the expression

$$G = gIL, \qquad (2)$$

where g is the SRS gain; I is the pump radiation intensity; and L is the gain length in the medium. It is also known [6–8] that the SRS threshold is reached at an increment value of ~25. For focused beams, it is commonly assumed [6–8, 30, 38] that the SRS gain length L is equal to the length of the confocal parameter of a beam with a Gaussian intensity profile in the cross section, or doubled Rayleigh length (1). In our case, the gain length of real picosecond radiation beams was determined for the first time from an increase in the SRS threshold

when part of the waist emerged from the water volume into the air. The beginning of an increase in the threshold intensity of the N-dependence means that the gain length in the exponent index decreases, i. e., the upper part of the waist begins to emerge from the water into the air. Then the distance from the waist to the surface is equal to half the gain length. Therefore, in our case, the entire gain length is (2 ×6) mm = 12 mm.

One can also see from Figure 4 that BSRS is suppressed in the water layer after the –3 mm mark. The next two steps (1 mm each) of approaching the waist to the surface without changing the pump pulse energy (1.3–1.5 mJ) are unexpectedly accompanied by the development of optical breakdown. Note that the breakdown threshold in the water volume was not reached even at the maximum pump pulse energy of ~16 mJ with the same experimental geometry.

It should also be noted that, in addition to SRS suppression, other features of the interaction of pump pulses with water near the surface were also observed. For example, the breakdown development was accompanied by water splashing in different directions with one preferred direction – flying away or spallation of part of the surface [39, 40] in the form of a drop along the beam axis into the geometric centre of the lens, which indicates an anisotropy of the pressure pulse of cylindrical symmetry with a noticeably larger magnitude along the axis beam. Hence it follows that the breakdown threshold (of multiphoton ionisation) [8] is reached in a region extended along the beam axis with a pump energy one or two orders of magnitude lower than the FSRS threshold. Next, the BSRS generation is restored at the same pump pulse energy, but after the waist is shifted by another 1 mm out of the water until it aligns with the surface and without breakdown, despite the minimum beam diameter and, accordingly, the maximum pump intensity at this energy. In this case, the generation of FSRS was observed at all waist positions, as well as during optical breakdown (see Fig. 4). The revealed fact indicates the development of FSRS at the leading edge of the pump pulse (57 ps) until the optical breakdown threshold is reached, as was observed earlier in the field of nanosecond pulses [8]. Hence it follows that the FSRS pulse duration will always be shorter than the pump pulse front, 15–20 ps, with subsequent compression as it propagates and amplifies in the pump field [38].

Thus, we have discovered a new phenomenon – BSRS suppression of picosecond (57 ps) pulses due to the development of an optical breakdown with a paradoxically low (~1.3 mJ) pump pulse energy upon moving the focal plane of a lens with a focal length of 83 mm in a layer 1–3 mm below the water surface. All the data obtained suggest that in the vicinity of the focal plane in a thin layer near the surface, energy density and intensity of all picosecond pulses (pump and SRS components) are self-consistently concentrated in time and space on the beam axis. It is physically obvious that the achievement of the breakdown threshold is ensured by the inclusion of all nonlinear optical processes that contribute to an increase in the total radiation intensity on the beam axis. Let us list the most significant processes in our case: these are electrostriction and self-focusing [41], the critical power (1.86 MW cm^{-2} [8]) of which is exceeded by more than an order of magnitude at an energy of 1 mJ for a 57 ps pulse, as well as the beam phase conjugation and compression of the BSRS pulse [7, 33, 34], which ensure maximum intensity in the beam waist near the surface. In this case, the waist's approach to the surface will increase the contribution of part of the high-intensity BSRS pulse with a shortened front, reflected from the surface towards the beam waist, which is amplified in the forward-direction pump field.

Regarding the Kerr lens and self-focusing, we note the following. Since the Kerr additive $n_2 I_p$ to the water refractive index $n = n_0 + n_2 I_p$ (n_0 and n_2 are the linear and nonlinear refractive indices, and I_p is the pump radiation intensity) is proportional to the optical field intensity I_p [6–8], a nonlinear Kerr lens with a maximum curvature on the beam axis in the threshold-free regime will be formed in the beam cross section. Note (see Fig. 4) that at a threshold energy of ~1.3 mJ, the power of a 57-ps pulse was ~23 MW. This value is one and a half orders of magnitude higher than the critical self-focusing power (1.86 MW) of a 100-ps second harmonic pulse (532 nm) of a neodymium laser in water. Given the high BSRS efficiency (up to 12%) and the reduction in the BSRS pulse duration when it moves towards the pump pulse, we can expect a multiple excess of the critical self-focusing power in the beam of the backward SRS wave [6].

It is essential that the BSRS beam phase conjugation [7, 33] ensures the superposition of counterpropagating beams (pump and BSRS waves) with maximum intensities in the waist region. It is physically clear that the nonlinear optical interaction of all optical fields near the waist as it approaches the water surface is modulated by picosecond pump pulses (57 ps) and shorter (due to compression) BSRS pulses.

An additional contribution to an increase in the total radiation intensity in the breakdown region comes from a fraction of the BSRS pulse, which is reflected from the water surface with a Fresnel coefficient (2%). The second passage of this part of the BSRS pulse through the Kerr lens in the waist direction is accompanied by an additional shortening of the pulse front simultaneously with its exponential amplification (2) and nonlinear beam compression. A slight removal of the waist from the surface ensures the encounter of BSRS pulses with short fronts, the total intensity of which reaches the breakdown threshold, and this region moves to the surface in the same direction as BSRS.

In addition, a special role of the water surface should be noted here, since the facts of modification of the structural forms of water near the surface are known: for example, the formation of ice-like structures in a water layer at room temperature [35], and also the fact that the order parameter of OH bonds near the water surface is higher than that in a quasi-liquid layer on the surface of a single crystal of hexagonal ice [36]. Of particular interest is the formation of a layer near the water interface, a so-called exclusive zone [42]. There is no doubt that the violation of the medium homogeneity due to the increased concentration of dissolved gases and the presence of structures and impurities in the water layer near the surface will reduce the breakdown threshold, which requires a separate study.

Despite a noticeable (almost an order of magnitude) increase in the BSRS threshold (~1.3 mJ) compared to that of FSRS (~0.17 mJ), when the focal plane is aligned with the surface (Fig. 4), the spectra of the SRS Stokes components differ insignificantly (Fig. 5).

One can see from Fig. 5 that both spectra have a characteristic feature: FSRS and BSRS generation develops simultaneously on two vibrational modes with frequencies of about 3400 and 3000 cm^{-1} inside the envelope of the OH band of water in spontaneous Raman scattering. Previously [17], the low-frequency band (~3000 cm^{-1}) that we found in the FSRS spectrum in water was interpreted as the result of four-wave mixing under conditions of noncollinear matching. To the

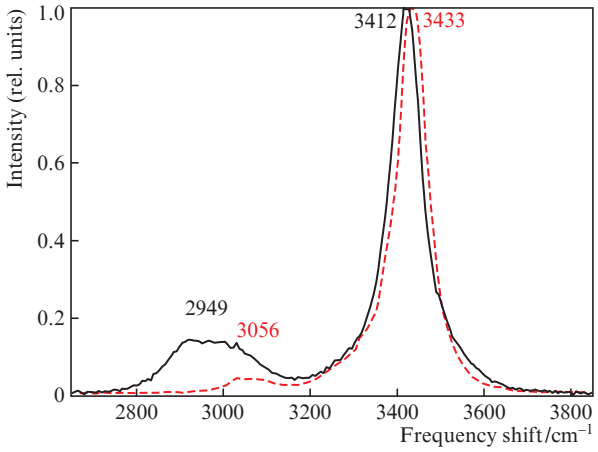

Figure 5. (Colour online) Spectra of SRS Stokes components in water in the forward (solid curve) and backward (dashed curve) directions when the focal plane is aligned with the surface.

best of our knowledge, we have for the first time implemented BSRS generation in water simultaneously in two vibrational modes. Taking into account the structural features of near-surface water layers [35, 36, 42], the interpretation of this result requires additional research. We believe that the observed red shift of the BSRS components (see Fig. 5) also reflects the asymmetry in the development of SRS generation in the lower half of the beam's caustic surface in water near the air–water interface.

4. Conclusions

Thus, backward SRS of radiation pulses with a duration of 57 ps at a wavelength of 532 nm was for the first time to our knowledge suppressed upon moving the beam waist near the water–air interface due to the development of optical breakdown with a paradoxical (more than an order of magnitude) threshold decrease of a still unclear nature. When the beam waist coincides with the water surface, BSRS generation is restored without increasing the pump pulse energy.

The results of measurements of the efficiency of pump radiation conversion into the 'forward–backward' SRS components (with increased efficiency for backward SRS) and the obtained threshold dependences indicate an asymmetry of the characteristics [13, 41] of BSRS and FSRS in water when the pump beam waist approaches the water–air interface from the water depth. In this case, for the first time, the FSRS gain length was determined when a real pump beam was focused into the volume of the medium, and BSRS generation in water was achieved simultaneously in two vibrational modes in the vicinity of 3400 and 3000 cm^{-1}. The physics of these revealed phenomena is not yet fully clear and requires further study.

Acknowledgements. The work was performed within the framework of the Belorussian Republican Foundation for Fundamental Research–Russian Foundation for Basic Research project F20R-013 (No. 20-52-00002 from the Russian side).

References

1. Franken P.A., Hill A.E., Peters C.W., Weinrich G. *Phys. Rev. Lett.*, **7**, 118 (1961).
2. Akhmanov S.A., Khokhlov R.V. *Problems of Nonlinear Optics. Electromagnetic Waves in Nonlinear Dispersive Media* (New York: Gordon and Breach, 1972; Moscow: Institute of Scientific Information, 1964).
3. Grasyuk A.Z., Efimkov V.F., Zubarev I.G., Mishin V.I., Smirnov V.G. *JETP Lett.*, **8**, 291 (1968) [*Pis'ma Zh. Eksp. Teor. Fiz.*, **8** (9), 474 (1968)].
4. Grasyuk A.Z. *Sov. J. Quantum Electron.*, **4** (3), 269 (1974) [*Kvantovaya Elektron.*, **1** (3), 485 (1974)].
5. Dzhotyan G.P., Dyakov Yu.E., Pershin S.M., Kholodnykh A.I. *Sov. J. Quantum Electron.*, **7** (6), 685 (1977) [*Kvantovaya Elektron.*, **4** (6), 1215 (1977)].
6. Shen Y.-R., in *Light Scattering in Solids. Topics in Applied Physics, V. 8*. Ed. by M. Cardona (Berlin, Heidelberg: Springer, 1975).
7. Boyd R.W. *Nonlinear Optics* (Academic Press, 4th edition, 2020).
8. Hafizi B., Palastro J.P., Penano J.R., Jones T.G., Johnson L.A., Helle M.H., Kaganovich D., Chen Y.H., Stamm A.B. *J. Opt. Soc. Am. B*, **33**, 2062 (2016).
9. Akhmanov S.A., Zhdanov B.V., Kovrigin A.I., Pershin S.M. *JETP Lett.*, **15**, 185 (1972) [*Pis'ma Zh. Eksp. Teor. Fiz.*, **15**, 266 (1972)].
10. Akhmanov S.A., Lyakhov G.A. *Sov. Phys. JETP*, **39**, 43 (1974) [*Zh. Eksp. Teor. Fiz.*, **66**, 96 (1974)].
11. Balakin A.V., Coutaz J.-L., Makarov V.A., Kotelnikov I.A., Peng Y., Solyankin P.M., Zhu Y., Shkurinov A.P. *Photonics Res.*, **7**, 678 (2019).
12. Pershin S.M., Grishin M.Ya., Lednev V.N., Chizhov P.A. *JETP Lett.*, **109**, 437 (2019) [*Pis'ma Zh. Eksp. Teor. Fiz.*, **109** (7), 447 (2019)].
13. Bolshov M.A., Golyaev Yu.I., Dneprovskiy V.S., Nurminsky I.I. *Sov. Phys. JETP*, **30**, 190 (1970) [*Zh. Eksp. Teor. Fiz.*, **57**, 346 (1970)].
14. Rahn O., Maier M., Kaiser W. *Opt. Commun.*, **1** (3), 109 (1969).
15. Pershin S.M., Grishin M.Ya., Lednev V.N., Garnov S.V., Bukin V.V., Chizhov P.A., Khodasevich I.A., Oshurko V.B. *Laser Phys. Lett.*, **15**, 035701 (2018).
16. Pershin S.M., Grishin M.Ya., Lednev V.N., Chizhov P.A., Orlovich V.A. *Opt. Lett.*, **44**, 5045 (2019).
17. Pershin S.M., Vodchits A.I., Khodasevich I.A., Grishin M.Ya., Lednev V.N., Orlovich V.A., Chizhov P.A. *Opt. Lett.*, **45**, 5624 (2020).
18. Pershin S.M., Shashkov E.V., Vorobiev N.S., Nikitin S.P., Grishin M.Ya., Komel'kov A.S. *Laser Phys. Lett.*, **17**, 115403 (2020).
19. Maier M., Kaiser W., Giordmaine J.A. *Phys. Rev. Lett.*, **17**, 1275 (1966).
20. Maier M., Kaiser W., Giordmaine J.A. *Phys. Rev.*, **177**, 580 (1969).
21. Alfano R.R., Zawadzkas G.A. *Phys. Rev. A*, **9**, 822 (1974).
22. Lin C.-H., Marshall B.R., Nelson M.A., Theobald J.K. *Appl. Opt.*, **17**, 2486 (1978).
23. Nikitin S.Yu., Sivashov D.A. *Vestnik Mosk. Univer., Ser. 3*, **33** (4), 66 (1992).
24. Kachinsky A.V., Kotaev G.G., Pilipovich I.V. *Quantum Electron.*, **22** (6), 507 (1992) [*Kvantovaya Elektron.*, **19** (6), 550 (1992)].
25. Kotaev G.G., Kruglik S.G., Orlovich V.A. *Quantum Electron.*, **22** (6), 504 (1974) [*Kvantovaya Elektron.*, **19** (6), 548 (1992)].
26. Apanasevich P.A., Gakhovich D.E., Grabchikov A.S., Kilin S.Ya., Kozich V.P., Kontsevoi B.L., Orlovich V.A. *Quantum Electron.*, **22** (9), 822 (1992) [*Kvantovaya Elektron.*, **19** (9), 884 (1992)].
27. Gorbunov V.A., Pivinsky E.G., Prilezhaev D.S. *Quantum Electron.*, **25** (3), 259 (1995) [*Kvantovaya Elektron.*, **22** (3), 275 (1995)].
28. Kolber T., Rozmus W., Tikhonchuk V.T. *Phys. Plasmas*, **2**, 256 (1995).
29. Tcherniega N., Sokolovskaia A., Kudriavtseva A.D., Barille R., Rivoire G. *Opt. Commun.*, **181**, 197 (2000).
30. Apanasevich P.A., D'yakov Yu.E., Kotaev G.G., Kruglik S.G., Nikitin S.Yu., Orlovich V.A. *Laser Phys.*, **3**, 131 (1993).
31. Mridha M.K., Novoa D., Russell P.St. *J. Opt.*, **5**, 570 (2018).
32. He G.S., Zhang F.-D., Shen Y., Cui Y. *J. Opt. Soc. Am. B*, **38**, 174 (2021).
33. Bespalov V.I., Pasmanik G.A. *Nelineinaya optika i adaptivnye lazernye sistemy* (Nonlinear Optics and Adaptive Laser Systems) (Moscow: Nauka, 1986) p. 134.

34. Sushchinsky M.M. *Vynuzhdennoe rasseyanie sveta* (Stimulated Light Scattering) (Moscow: Nauka, 1985) p. 176.
35. Jinesh K.B., Frenken J.W.M. *Phys. Rev. Lett.*, **101**, 036101 (2008).
36. Wei X., Miranda P.B., Shen Y.R. *Phys. Rev. Lett.*, **86**, 1554 (2001).
37. Yui H. *Anal. Bioanal. Chem.*, **397**, 1181 (2010).
38. Akhmanov S.A., Koroteev N.I. *Metody nelineinoi optiki v spektroskopii rasseyaniya sveta* (Nonlinear Optics Methods in Light Scattering Spectroscopy) (Moscow: Nauka, 1981) p. 544.
39. Mordkovich V.Z. *Khimiya i Zhizn'*, (2), 8 (2003).
40. Volkov M., Kishalov A., Orlov N., Serebryakov V., Smirnov V., Filatov A. *Fotonika*, **45**, 34 (2014).
41. Shen Y.R. *Phys. Lett.*, **20**, 378 (1966).
42. Pollack G.H. *The Fourth Phase of Water: Beyond Solid, Liquid and Vapor* (Ebner and Sons, 2013).